PROCEEDINGS OF SCIENCE

Recent Vector Boson Scattering results from CMS

K. Sandeep[a]
for the CMS Collaboration

[a] *Panjab University, Chandigarh, India*

E-mail: sandeep.kaur.hundal@cern.ch

The ultimate test of the Higgs mechanism in Electroweak Symmetry Breaking (EWSB) lies in the vector boson scattering (VBS) processes. In this contribution, we present recent vector boson scattering measurements involving W, Z and photon combinations in proton-proton collisions at the LHC. The data samples are collected at a center-of-mass energy of 13 TeV with the CMS detector at the LHC. The analyses are performed in the fully leptonic final states. Recent results related to same sign WW, WZ, polarized WW, ZZ and Wγ scattering are discussed.

40th International Conference on High Energy physics - ICHEP2020
July 28 - August 6, 2020
Prague, Czech Republic (virtual meeting)

PoS(ICHEP2020)342

1. Introduction

The observation of the Higgs boson with a mass of about 125 GeV by the ATLAS and CMS experiments is a triumph of the standard model (SM) that has opened a new era in particle physics. Within the current uncertainties, the newly found particle is consistent with the SM expectations. However, an ultimate test of the Higgs mechanism in Electroweak Symmetry Breaking (EWSB) lies in the vector boson scattering (VBS) process. Extensive VBS measurements are covered by the CMS collaboration. The focus of this report is on a selection among the most recent public results.

One of the recent analyses [1] measures both $W^{\pm}W^{\pm}jj$ and WZjj electroweak production modes by fitting simultaneously several distributions sensitive to these processes. The second analysis [2] corresponds to first search for scattering of polarized same-sign W boson pairs. The third analysis [3] presents the evidence of the electroweak (EW) production of two jets in association with two Z bosons, where both Z bosons decay into electrons or muons. All three analyses are based on a data sample corresponding to an integrated luminosity of 137.4 fb^{-1}. The last analysis [4] that is being reported corresponds to the measurement of the EW production of a W boson and a photon in association with two jets , where the W boson decays leptonically and is based on a data sample corresponding to an integrated luminosity of 35.9 fb^{-1}.

A detailed description of the CMS detector, together with a definition of the coordinate system and the relevant kinematic variables, is reported in [5].

2. Overview of VBS measurement

The typical VBS topology at hadron colliders features two energetic forward-backward jets in opposite hemisphere with large dijet mass and rapidity separation, and two vector bosons (VV) produced centrally. The experimental analysis involves selection of VV events with VBS-like jets and then estimating non-VV backgrounds. There are two types of non-VV backgrounds - nonprompt or fake background and prompt background. Nonprompt background is selected due to misidentification of experimental backgrounds and it is estimated from data-driven techniques. The prompt background is the irreducible background that is selected without any misidentification and is estimated from monte carlo simulations. After the estimation of background and considering systematic and statistical uncertainties, various measurements are carried out, e.g. inclusive and differential cross section measurements and search for anomalous quartic gauge couplings (aQGCs) etc.

3. Recent Results

The focus of this section is to showcase results of the four of the recent public VBS results.

3.1 Same-sign WW and WZ scattering

It is the first simultaneous same-sign WW and WZ analysis that is carried out using full Run II CMS data. Kinematic selection cuts are applied along with VBS cuts to get signal events dominance over background events. A multivariate analysis is carried out for WZ to enhance WZ EWK

production w.r.t large WZ QCD production. Statistical analysis is done by simultaneously fitting signal yields in WW and WZ signal regions as well as background yields in control regions in order to assess normalization from data. There are many systematic uncertainties, but the analysis is dominated by statistical uncertainty. An observation of electroweak production of WZ boson pairs is reported with an observed (expected) significance of 6.8 (5.3) standard deviations. Inclusive cross section measurements for the EW WW, EW+QCD WW, EW WZ, QCD WZ, and EW+QCD WZ processes are performed and they came out to be comparable to the theoretical predictions. Absolute and normalized WW differential production cross section measurements in bins of m_{jj} for WW production and WZ production is shown in Fig. 1. Stringent limits are set in the framework of effective field theory (EFT), with and without consideration of tree-level unitarity violation, on the dimension-8 operators, as shown in Tables 1 and 2, respectively. The clipping method [6] is used for the first time in the CMS analysis to set the most conservative limits considering the region of validity of EFT.

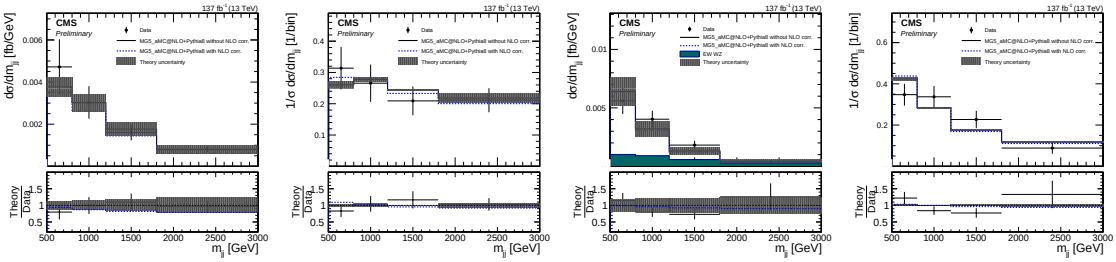

Figure 1: The measured absolute and normalized $W^{\pm}W^{\pm}$ (first and second) fiducial cross section measurements in bins of m_{jj} and similar for WZ (third and fourth) fiducial cross section measurements. Taken from [1]

	Observed ($W^{\pm}W^{\pm}$) (TeV^{-4})	Expected ($W^{\pm}W^{\pm}$) (TeV^{-4})	Observed (WZ) (TeV^{-4})	Expected (WZ) (TeV^{-4})	Observed (TeV^{-4})	Expected (TeV^{-4})
f_{T0}/Λ^4	[-0.28, 0.31]	[-0.36, 0.39]	[-0.62, 0.65]	[-0.82, 0.85]	[-0.25, 0.28]	[-0.35, 0.37]
f_{T1}/Λ^4	[-0.12, 0.15]	[-0.16, 0.19]	[-0.37, 0.41]	[-0.49, 0.55]	[-0.12, 0.14]	[-0.16, 0.19]
f_{T2}/Λ^4	[-0.38, 0.50]	[-0.50, 0.63]	[-1.0 , 1.3]	[-1.4, 1.7]	[-0.35, 0.48]	[-0.49, 0.63]
f_{M0}/Λ^4	[-3.0, 3.2]	[-3.7, 3.8]	[-5.8, 5.8]	[-7.6, 7.6]	[-2.7, 2.9]	[-3.6, 3.7]
f_{M1}/Λ^4	[-4.7, 4.7]	[-5.4, 5.8]	[-8.2, 8.3]	[-11, 11]	[-4.1, 4.2]	[-5.2, 5.5]
f_{M6}/Λ^4	[-6.0, 6.5]	[-7.5, 7.6]	[-12, 12]	[-15, 15]	[-5.4, 5.8]	[-7.2, 7.3]
f_{M7}/Λ^4	[-6.7, 7.0]	[-8.3, 8.1]	[-10, 10]	[-14, 14]	[-5.7, 6.0]	[-7.8, 7.6]
f_{S0}/Λ^4	[-6.0, 6.4]	[-6.0, 6.2]	[-19, 19]	[-24, 24]	[-5.7, 6.1]	[-5.9, 6.2]
f_{S1}/Λ^4	[-18, 19]	[-18, 19]	[-30, 30]	[-38, 39]	[-16, 17]	[-18, 18]

Table 1: Observed and expected lower and upper 95% CL limits on the parameters of the quartic operators in $W^{\pm}W^{\pm}$ and WZ channels, obtained without using any unitarization procedure. The last two columns show the observed and expected limits for the combination of the $W^{\pm}W^{\pm}$ and WZ channels. Taken from [1]

3.2 Polarized same-sign WW scattering

It is the first measurement of EW production cross section of polarized $W^{\pm}W^{\pm}$, an analysis of its kind with real data and also one of the high profile analyses for HL- LHC. The event selection and background estimation is same as for the unpolarized WW VBS analysis. Boosted Decision Tree (BDT) techniques are used to separate between the polarized scattering processes by exploiting the kinematic differences. An observed (expected) 95% CL upper limit on the production cross section

	Observed ($W^{\pm}W^{\pm}$) (TeV^{-4})	Expected ($W^{\pm}W^{\pm}$) (TeV^{-4})	Observed (WZ) (TeV^{-4})	Expected (WZ) (TeV^{-4})	Observed (TeV^{-4})	Expected (TeV^{-4})
f_{T0}/Λ^4	[-1.5, 2.3]	[-2.1, 2.7]	[-1.6, 1.9]	[-2.0, 2.2]	[-1.1, 1.6]	[-1.6, 2.0]
f_{T1}/Λ^4	[-0.81, 1.2]	[-0.98, 1.4]	[-1.3, 1.5]	[-1.6, 1.8]	[-0.69, 0.97]	[-0.94, 1.3]
f_{T2}/Λ^4	[-2.1, 4.4]	[-2.7, 5.3]	[-2.7, 3.4]	[-4.4, 5.5]	[-1.6, 3.1]	[-2.3, 3.8]
f_{M0}/Λ^4	[-13, 16]	[-19, 18]	[-16, 16]	[-19, 19]	[-11, 12]	[-15, 15]
f_{M1}/Λ^4	[-20, 19]	[-22, 25]	[-19, 20]	[-23, 24]	[-15, 14]	[-18, 20]
f_{M6}/Λ^4	[-27, 32]	[-37, 37]	[-34, 33]	[-39, 39]	[-22, 25]	[-31, 30]
f_{M7}/Λ^4	[-22, 24]	[-27, 25]	[-22, 22]	[-28, 28]	[-16, 18]	[-22, 21]
f_{S0}/Λ^4	[-35, 36]	[-31, 31]	[-83, 85]	[-88, 91]	[-34, 35]	[-31, 31]
f_{S1}/Λ^4	[-100, 120]	[-100, 110]	[-110, 110]	[-120, 130]	[-86, 99]	[-91, 97]

Table 2: Observed and expected lower and upper 95% CL limits on the parameters of the quartic operators in $W^{\pm}W^{\pm}$ and WZ channels by cutting the EFT expansion at the unitarity limit. Taken from [1]

for longitudinally polarized same-sign WW boson pairs of 1.17 (0.88) fb is reported with the helicity eigen-states defined in the WW center-of-mass reference frame. The electroweak production of the WW boson pairs where at least one of the W bosons is longitudinally polarized, is measured with an observed (expected) significance of 2.3 (3.1) σ. Results are also reported with the polarizations defined in the parton-parton center-of-mass reference frame. The measured cross section values agree with the theoretical predictions within uncertainties as shown in Fig. 2.

Process	$\sigma\,\mathcal{B}$ (fb)	Theoretical prediction (fb)
$W^{\pm}_{L}W^{\pm}_{L}$	$0.32^{+0.42}_{-0.40}$	0.44 ± 0.05
$W^{\pm}_{X}W^{\pm}_{T}$	$3.06^{+0.51}_{-0.48}$	3.13 ± 0.35
$W^{\pm}_{L}W^{\pm}_{X}$	$1.20^{+0.56}_{-0.53}$	1.63 ± 0.18
$W^{\pm}_{T}W^{\pm}_{T}$	$2.11^{+0.49}_{-0.47}$	1.94 ± 0.21

Process	$\sigma\,\mathcal{B}$ (fb)	Theoretical prediction (fb)
$W^{\pm}_{L}W^{\pm}_{L}$	$0.24^{+0.40}_{-0.37}$	0.28 ± 0.03
$W^{\pm}_{X}W^{\pm}_{T}$	$3.25^{+0.50}_{-0.48}$	3.32 ± 0.37
$W^{\pm}_{L}W^{\pm}_{X}$	$1.40^{+0.60}_{-0.57}$	1.71 ± 0.19
$W^{\pm}_{T}W^{\pm}_{T}$	$2.03^{+0.51}_{-0.50}$	1.89 ± 0.21

Figure 2: Measured fiducial cross sections for the $W^{\pm}_{L}W^{\pm}_{L}$ and $W^{\pm}_{X}W^{\pm}_{T}$ processes and for the $W^{\pm}_{L}W^{\pm}_{X}$ and $W^{\pm}_{T}W^{\pm}_{T}$ processes for the helicity eigenstates defined in the $W^{\pm}W^{\pm}$ center-of-mass frame(left table) and the parton-parton center-of-mass frame(right table). Taken from [2]

3.3 ZZ scattering

A search for the electroweak production of two Z bosons in the four-lepton final state in association with two jets is presented. A discriminant (K_D) based on a matrix element likelihood approach (MELA) is used to extract the signal significance and to measure the cross sections for the EW and the EW+QCD production of the 4l+jj final state in a fiducial volume. Fig. 3 presents the m_{jj} and $|\Delta\eta_{jj}|$ distributions in the ZZjj inclusive region. The distribution of the K_D discriminant for all events in the $ZZjj$ inclusive selection is shown in Fig. 3. It is confirmed that the K_D discriminant kas greater power to capture differences between the kinematical distributions of signal and background events. The electroweak production of two jets in association with a pair of Zbosons is measured with an observed (expected) significance of 4.0 (3.5) standard deviations. The measured fiducial cross section is $\sigma_{fid} = 0.33^{+0.11}_{-0.10}(stat)^{+0.04}_{-0.03}(syst)$ fb, which is consistent with the SM prediction. Constraints on anomalous quartic gauge couplings are also presented. Table 3 lists the individual lower and upper limits obtained by setting all other anomalous couplings to zero.

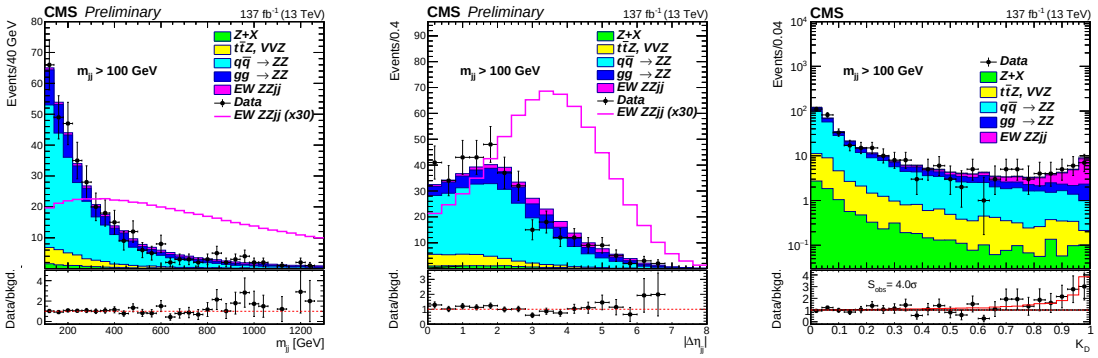

Figure 3: Distribution of m_{jj}(left) and $|\Delta\eta_{jj}|$ (middle) for events satisfying the ZZjj inclusive selection and distribution of the matrix-element discriminant with fit normalizations for events satisfying the ZZjj inclusive selection. Taken from [3]

Coupling	Exp. lower	Exp. upper	Obs. lower	Obs. upper	Unitarity bound
f_{T0}/Λ^4	−0.37	0.35	−0.24	0.22	2.4
f_{T1}/Λ^4	−0.49	0.49	−0.31	0.31	2.6
f_{T2}/Λ^4	−0.98	0.95	−0.63	0.59	2.5
f_{T8}/Λ^4	−0.68	0.68	−0.43	0.43	1.8
f_{T9}/Λ^4	−1.5	1.5	−0.92	0.92	1.8

Table 3: Expected and observed limits of the 2σ CL intervals on the couplings of the quartic operators T0, T1, and T2, as well as the neutral current operators T8 and T9. All coupling parameter limits are in TeV^{-4}, while the unitarity bounds are in TeV. Taken from [3]

3.4 Wγ scattering

A measurement of the electroweak (EW) production of a W boson and a photon in association with two jets in proton-proton collisions, where the W boson decays leptonically, is presented. The statistical analysis of the event yields is performed with a fit to the (m_{jj}, $m_{l\gamma}$) two-dimensional distributions, in order to quantify the significance of the observation of the EW production of Wγ boson pairs. The data in the low m_{jj} control region are fit simultaneously with the data in the signal region. The low m_{jj} control region and the signal region are divided into four bins for the different channels (electron barrel,electron endcap, muon barrel and muon endcap), but only one overall m_{jj} bin for the control region. Fig. 4 shows the post-fit (i.e., after the simultaneous fit) 2D distributions. The observed significance is 4.9 σ, whereas significance of 4.6 σ is expected based on the SM. After combining with the 8 TeV result, the observed (expected) significance is 5.3 (4.8) σ. This constitutes the first observation of electroweak Wγ production in pp collisions. A fiducial cross section is extracted using the same m_{jj}-$m_{l\gamma}$ binning as for the calculation of the significance, and through the same simultaneous fit used in the control region. The cross section measurement is consistent with SM predictions. The cross section measured in the fiducial region is 20.4 ± 4.5 fb and the total cross section for EW + QCD Wγ production in association with 2 jets in the same fiducial region is measured to be 108 ± 16 fb.

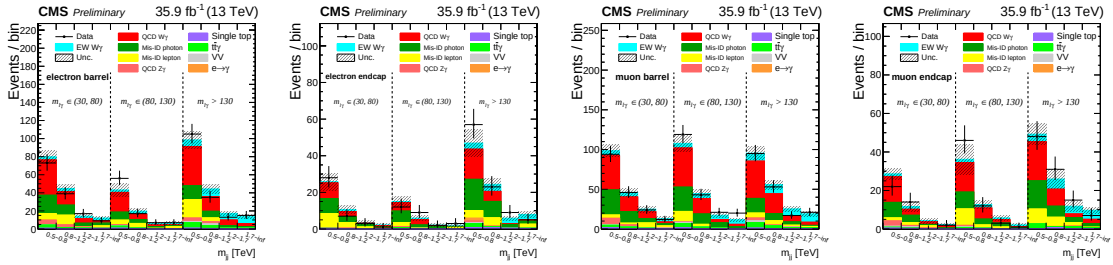

Figure 4: The 2D distributions used in the fit for the signal strength of EW Wγ + 2 jets in the electron barrel (first), electron endcap (second), muon barrel (third), and muon endcap (last). Taken from [4]

4. Summary

Latest CMS results on EW scattering of WW, WZ, ZZ and Wγ are reported. Inclusive and differential cross sections measurements are carried out and stringent limits on aQGCs under consideration of unitarity constraints are set for the first time. This is just the starting point of a long physics program.

References

[1] CMS Collaboration, Phys. Lett. B 809 (2020) 135710.

[2] CMS Collaboration, CMS Physics Analysis Summary CMS-PAS-SMP-20-006, arXiv:2009.09429, 2020, https://cds.cern.ch/record/2724972.

[3] CMS Collaboration, CMS Physics Analysis Summary CMS-PAS-SMP-20-001, 2020, https://cds.cern.ch/record/2718812.

[4] CMS Collaboration, CMS Physics Analysis Summary CMS-PAS-SMP-19-008, 2020, http://cds.cern.ch/record/2718822.

[5] CMS Collaboration, JINST 3, S08004 (2008).

[6] J. Kalinowski et al., Eur. Phys. J. C78(2018) 403.